Oct 29th, 12:00 AM - Oct 30th, 12:00 AM

International Conference on Mechatronic

University for Business and Technology - UBT

Leadership and Innovation

Education | Research | Training | Consulting | Certification

PROCEEDINGS

11th UBT ANNUAL INTERNATIONAL CONFERENCE

INTERNATIONAL CONFERENCE ON MECHATRONICS, SYSTEM ENGINEERING AND ROBOTICS

29-30 OCTOBER

UBT Innovation Campus

Proceedings of the 11th Annual International Conference on Mechatronics, System Engineering and Robotics

Edited by
Edmond Hajrizi

Conference Book of Proceedings International Conference Pristina

ISBN 978-9951-550-87-1

International Conference on Business, Technology and Innovation Pristina, 29-30
Editor: Edmond Hajrizi

Publisher, UBT

Editor Speech of IC - BTI

International Conference is the 11th international interdisciplinary peer reviewed conference which publishes works of the scientists as well as practitioners in the area where UBT is active in Education, Research and Development. The UBT aims to implement an integrated strategy to establish itself as an internationally competitive, research-intensive institution, committed to the transfer of knowledge and the provision of a world-class education to the most talented students from all backgrounds. It is delivering different courses in science, management and technology. This year we celebrate the 21th Years Anniversary. The main perspective of the conference is to connect scientists and practitioners from different disciplines in the same place and make them be aware of the recent advancements in different research fields, and provide them with a unique forum to share their experiences. It is also the place to support the new academic staff for doing research and publish their work in international standard level. This conference consists of sub conferences in different fields: - Management, Business and Economics - Humanities and Social Sciences (Law, Political Sciences, Media and Communications) - Computer Science and Information Systems - Mechatronics, Robotics, Energy and Systems Engineering - Architecture, Integrated Design, Spatial Planning, Civil Engineering and Infrastructure - Life Sciences and Technologies (Medicine, Nursing, Pharmaceutical Sciences, Phycology, Dentistry, and Food Science),- Art Disciplines (Integrated Design, Music, Fashion, and Art). This conference is the major scientific event of the UBT. It is organizing annually and always in cooperation with the partner universities from the region and Europe. In this case as partner universities are: University of Tirana – Faculty of Economics, University of Korca. As professional partners in this conference are: Kosovo Association for Control, Automation and Systems Engineering (KA – CASE), Kosovo Association for Modeling and Simulation (KA – SIM), Quality Kosovo, Kosovo Association for Management. This conference is sponsored by EUROSIM - The European Association of Simulation. We have to thank all Authors, partners, sponsors and also the conference organizing team making this event a real international scientific event. This year we have more application, participants and publication than last year.

Congratulation!

Edmond Hajrizi, Rector of UBT and Chair of IC - BTI

CONTENT

Watermelon seeds germination study by shortwave infrared-based hyperspectral imaging techniques

Giuseppe Bonifazi[1,2 *], Riccardo Gasbarrone[1], Silvia Serranti[1,2], Kliton Bylykbashi[3]

[1] Department of Chemical Engineering Materials Environment,
Sapienza University of Rome, Italy
[2] Research Center for Biophotonics, Sapienza University of Rome,
Polo Pontino, Italy
[3] UBT – Higher Education Institution, Lagjja Kalabria, 10000 Pristina, Kosovo

giuseppe.bonifazi@uniroma1.it, riccardo.gasbarrone@uniroma1.it
silvia.serranti@uniroma1.it
kliton.bylykbashi@ubt-uni.net

Abstract. The germination capability of watermelon (*Citrullus Lanatus*) represents the proportion of seeds producing healthy seedlings within the parameters and time frames specified by the approved techniques of analysis. Rapid and non-invasive analytical processes for seed quality control must be established in order to guarantee the quality and germination of seed production up until the point of use. In this scenario, Near Infrared (NIR)-based HyperSpectral Imaging (HSI) represents an optimal solution for quality control applications in different sectors. The purpose of this study was to explore the utilization of methods based on the use of HyperSpectral Imaging (HSI) in the Short-Wave Infrared (SWIR) spectral region (1000–2500 nm) to test the germinability of watermelon seeds. A Partial Least Squares–Discriminant Analysis (PLS-DA) model was built in order to recognize non-viable seeds from viable ones. The obtained classification results are promising, reaching a sensitivity of 0.72 and a specificity of 0.98 for not germinated seed.

.

Keywords: Seeds; Germinability; Watermelon; HyperSpectral Imaging; Short-Wave Infrared; HIS; SWIR; Partial Least Squares–Discriminant Analysis.

1 Introduction

The edible fruit of the flowering plant species known as watermelon (*Citrullus lanatus*) belongs to the Cucurbitaceae family. It is a scrambling, trailing vine-like plant with more than a thousand different varieties of fruit that are widely farmed throughout the world. Since the watermelon is an annual crop, it will complete its entire life cycle in one growing season, including germination, reproduction and death. A single watermelon plant can produce viable seeds, however many seeds of the fruit could not germinate. In this context, a crucial step in the quality certification process of this variety is the seed analysis. The seeds must meet particular conditions in relation to their identification and varietal purity, their biological and physical status in order to be certified and subsequently placed on the market. The germination analysis determines the proportion of pure seeds that can sprout normally, i.e., seedlings whose fundamental structures have a balanced and healthy development and are able to grow, under ideal cultivation conditions, plants that can complete their entire vegetative and reproductive cycle. The percentage of seeds, developing healthy seedlings within the parameters and time frames defined by the approved methods of analysis, is represented by the germination capability on the analysis certificates. The germination tests have a variable duration depending on the species, ranging from a few days up to a month. In more detail, watermelon seeds germinate in 4 to 12 days. To ensure the quality and germination of seeds right up until the moment of use, it is necessary to establish rapid and non-invasive quality control analytical procedures.

In recent years, multispectral and hyperspectral imaging techniques in the visible (450 - 950 nm) and near infrared (950-1650 nm) have been studied, with the specific aim: i) to evaluate seeds quality in a non-destructive and non-invasive way and to select seeds on the basis of their vitality [1, 2], ii) to evaluate seeds deterioration and, finally, iii) to identify abiotic [3-5] and biotic[6] damage in seeds. There are also several studies in the literature on the application of infrared spectroscopy to predict soybean germination [7] and predict the germination rate of tomato seeds [8].

This study was carried out to assess whether methods based on the utilization of HyperSpectral Imaging (HSI) in the Short-Wave InfraRed (SWIR) spectral region (1000-2500 nm) could be used to identify watermelon (*Citrullus Lanatus*) seeds that could or could not germinate. Firstly, watermelon seeds were analyzed to evaluate their germinability using the standard approach (seed germinated after one month from the acquisition). Starting from hyperspectral images in the SWIR, Partial Least Squares – Discriminant Analysis (PLS-DA) classification models were calibrated and validated to recognize watermelon non-viable seeds (sowed plant dead at a distance of one month from the acquisition) from viable seeds.

2 Material and methods

2.1 Sample preparation and data acquisition

The analyzed seed samples were purchased from a local wholesale company of gardening supplies (Orto Strabilia, Latina, Italy). In more detail, a set of 100 watermelon seeds (*Citrullus Lanatus*) was analyzed (Figure 1a). The seeds were arranged in a plate in order to acquire the hyperspectral image.
The SisuCHEMA XL^{TM} (Specim, Finland) device, operating in the wavelength range of 1000-2500 nm with a spectral resolution of 6.2 nm, was utilized to acquire the hyperspectral image in reflectance mode. Acquisition optics have a 31-mm aperture, allowing for the capture of images with a 50 mm width by 18 mm/s scanning speed. A hyperspectral image showing the 100 seeds of watermelon seeds was captured.

2.2 Data preparation and germinability evaluation

Acquired hyperspectral image (Figure 1b) was imported into MATLAB Environment (MATLAB R2017b ver. 9.3.0.). Data processing and chemometric analyzes have been carried out within PLS_toolbox (ver. 8.6.0.) and MIA_toolbox (ver. 3.0.5) tollboxes

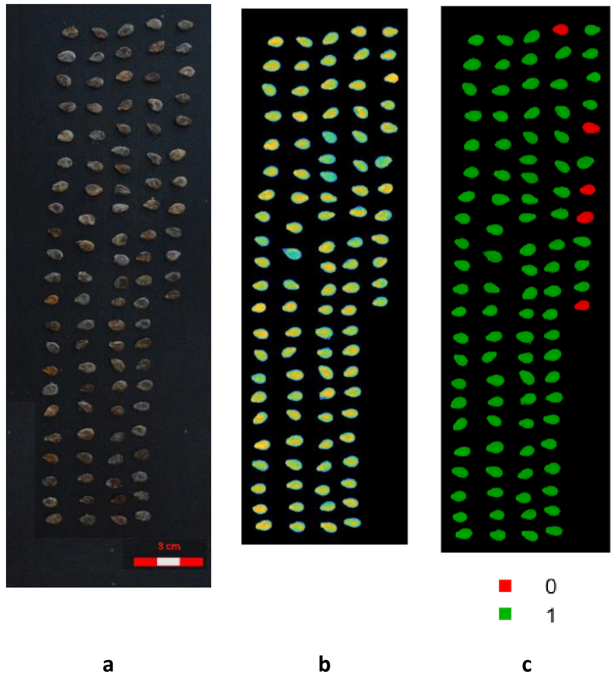

Fig 1. Watermelon (Citrullus Lanatus) seeds: RGB image of the samples (a), Hyperspectral image (b) and dataset with set classes (c). Legend notes: “0” = not germinated, “1” = germinated.

Table 1. Number of germinated and non-germinated watermelon seeds. (*) “0” = non-viable / non-germinated (seed not germinated one month after acquisition); “1” = viable / germinated (seed germinated one month after acquisition).

Condition*	0	1
Total	5	95
Calibration set	4	81
Validation set	1	14

running inside MATLAB. The background of the hyperspectral image was excluded and classes were set.

The viability classes were assessed by visual inspection one month after acquisition. The classes set on the image (Figure 1c) are ‘0’ = non-viable / non-germinated and ‘1’ = viable / germinated. In Table 1 are shown the numbers of germinated and non-germinated seeds one month after their acquisition and subdivision.

The dataset has been then divided into a calibration set (containing about 70% of the particles for each class) and a validation set (containing about 30% of the particles for each class). The calibration and validation sets for the watermelon dataset are shown in Figure 2.

2.3 Data preparation and germinability evaluation

Different combinations of spectral data preprocessing algorithms were tested. Among these, the chosen combination sequence of pre-processing algorithms is the following:

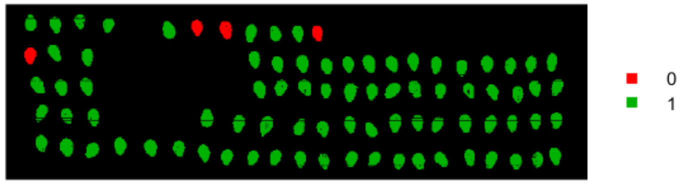

Calibration

Validation

Fig. 2. Calibration set and validation set for watermelon (Citrullus Lanatus) dataset. Legend notes: “0” = not germinated, “1” = germinated.

Generalized Least Squares weighting (GLSW, performed on the classes, with alpha = 0.0001), Savitzky–Golay Smoothing and Mean Center (MC) [9, 10].

Principal Component Analysis (PCA), that is a mathematical algorithm that reduces data dimensionality while retaining the majority of data variation, was performed on calibration datasets to explore intra-class variability and for outliers’ identification [11]. The outliers were identified and excluded from subsequent analyzes.

2.4 Partial Least Squares - Discriminant Analysis

The Partial Least Squares – Discriminant Analysis (PLS-DA) is a flexible algorithm that can be used for both predictive and descriptive modeling [12, 13].

PLS-DA was chosen as classification method and applied to evaluate the predictive ability of SWIR spectra to classify the studied samples, that is to distinguish the two classes: "0" = non-viable / non-germinated seed (non-germinated seed one month after acquisition) and "1" = viable / germinated seed (germinated seed one month after acquisition).

Venetian blinds algorithm was used to evaluate the complexity of the model and choose an adequate number of latent variables. The PLS-DA model was built from the calibration dataset and validated by applying it to the validation dataset.

3 Results and discussion

3.1 Exploratory analysis

The average reflectance spectra of the calibration dataset are shown in Figure 3. Main differences between the average reflectance spectra of viable and not-viable seeds occurs around 1500 – 1800 nm and 2000-2400 nm.

3.2 Classification

The results of the PLS-DA classifications in terms of *Sensitivity* and *Specificity* for the

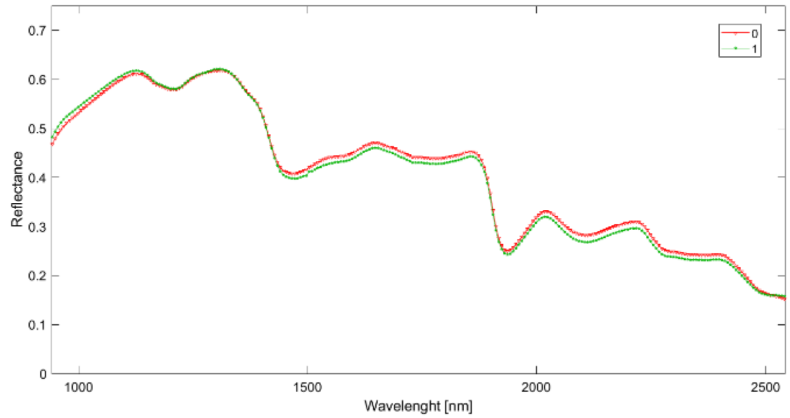

Fig. 3. Average reflectance spectra of the germination classes of the watermelon seeds. Legend notes: 0 = not germinated, 1 = germinated.

Table 2. *Sensitivity* and *Specificity* in calibration (Cal), cross-validation (CV) and prediction (Pred) for the PLS-DA model discriminating the germination classes of watermelon seeds. (*) "0" = non-viable / non-germinated (seed not germinated one month after acquisition); "1" = viable / germinated (seed germinated one month after acquisition).

Class*	(0)	(1)
Sensitivity (Cal)	0.963	0.909
Specificity (Cal)	0.909	0.963
Sensitivity (CV)	0.825	0.813
Specificity (CV)	0.813	0.825
Sensitivity (Pred)	0.725	0.981
Specificity (Pred)	0.981	0.725

watermelon seeds are summarized in Table 2. While the prediction maps for calibration and validation sets are shown in Figure 3. From what can be deduced from the classification results, through PLS-DA it is possible to recognize (in prediction) all the non-germinating seeds (Figure 4).

4 Conclusions

The results obtained show how it is possible to recognize non-viable seeds of watermelon (*Citrullus Lanatus*) using hyperspectral techniques in the short-wave infrared range (1000-2500 nm). SWIR-HSI techniques can be applied to test the germinability of watermelon seeds. The results of the classification are promising and opens the door for further germination studies using the same techniques on other varieties. Further investigations for the development of a novel classification models should be carried out on different kind of seeds.

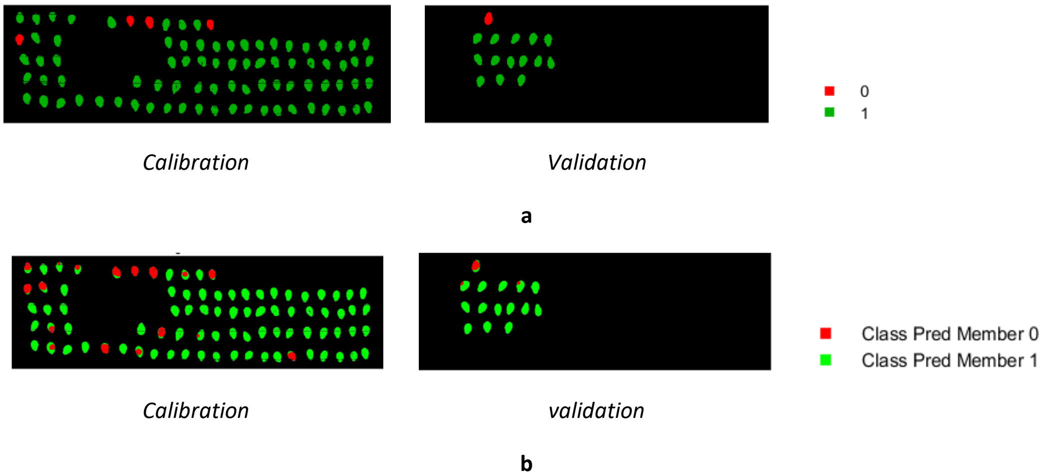

Fig. 4. Calibration set and validation set (a) prediction maps in calibration and validation (b) for watermelon seeds. Legend notes: 0 = not germinated, 1 = germinated.

References

1. Olesen, M.H., J.M. Carstensen, and B. Boelt, Multispectral imaging as a potential tool for seed health testing of spinach (Spinacia oleracea L.). Seed Science and Technology, 2011. 39(1): p. 140-150.
2. Olesen, M.H., et al., Classification of viable and non-viable spinach (Spinacia oleracea L.) seeds by single seed near infrared spectroscopy and extended canonical variates analysis. Journal of Near Infrared Spectroscopy, 2011. 19(3): p. 171-180.
3. Wang, D., M. Ram, and F. Dowell, Classification of damaged soybean seeds using near–infrared spectroscopy. Transactions of the ASAE, 2002. 45(6): p. 1943.
4. Agelet, L.E., et al., Feasibility of near infrared spectroscopy for analyzing corn kernel damage and viability of soybean and corn kernels. Journal of Cereal Science, 2012. 55(2): p. 160-165.
5. Jia, S., et al., Feasibility of analyzing frost-damaged and non-viable maize kernels based on near infrared spectroscopy and chemometrics. Journal of Cereal Science, 2016. 69: p. 145-150.
6. Pasikatan, M. and F. Dowell, Sorting systems based on optical methods for detecting and removing seeds infested internally by insects or fungi: a review. 2001.
7. Al-Amery, M., et al., Near-infrared spectroscopy used to predict soybean seed germination and vigour. Seed Science Research, 2018. 28(3): p. 245-252.
8. Tao, W. and W. Xiaofei. Study on germination of tomato seed based on near-infrared spectroscopy. in 2013 IEEE 11th International Conference on Electronic Measurement & Instruments. 2013. IEEE.
9. Savitzky, A. and M.J. Golay, Smoothing and differentiation of data by simplified least squares procedures. Analytical chemistry, 1964. 36(8): p. 1627-1639.
10. Rinnan, Å., F. Van Den Berg, and S.B. Engelsen, Review of the most common pre-processing techniques for near-infrared spectra. TrAC Trends in Analytical Chemistry, 2009. 28(10): p. 1201-1222.
11. Wold, S., K. Esbensen, and P. Geladi, Principal component analysis. Chemometrics and intelligent laboratory systems, 1987. 2(1-3): p. 37-52.
12. Ballabio, D. and V. Consonni, Classification tools in chemistry. Part 1: linear models. PLS-DA. Analytical Methods, 2013. 5(16): p. 3790-3798.
13. Wise, B.M., et al., Chemometrics tutorial for PLS_Toolbox and Solo. Eigenvector Research, Inc, 2006. 3905: p. 102-159.

Static Analysis of Welded Bead of Street Lighting Construction

Fidan Smaili[1*], Armend Sylaj[1], Besart Berisha[2], Afrim Gjelaj[2], Drilon Beqiri[3]

[1]University for Business and Technology, Faculty of Mechatronics Management

[2]University of Prishtina, Faculty of Mechanical Engineering

[3]University ''Isa Boletini'' Mitrovicë, Faculty of Mechanical and Computer Engineering

e-mail: fidan.smaili@ubt-uni.net

Abstract

Public lighting is for sure of unique importance for our safety, but it is also crucial to ensure that the street lighting construction does not fail due to static load or when unpredicted additional loads (like wind storms) could potentially be subjected to. To ensure that the failure of the street lighting construction will not happen, the mechanical properties of the weld joint should be known. Tensile test and hardness measurements were used as destructive examination methods and visual inspection using the welding gauge as a nondestructive examination for measurement of reinforcement and weld size. Finally, static analysis is performed by simulation in SolidWorks software, and the results were compared with the experimental test. Based on the results should be no concern, if the inspection is done properly before, during, and after welding by IWS (International Welding Specialist) personnel and in accordance with WPS (Welding Procedure Specification) and PQR (Procedure Qualification Record).

Keywords: Static analysis, Weld bead, Heat Affected Zone, Mechanical properties, SolidWorks software.

1 Introduction

It is estimated that over 50% of global domestic and engineering products contain welded joints and in Europe the welding industry has traditionally supported a diverse set of companies across the shipbuilding, pipeline, automotive, aerospace, defense and construction sectors etc. Since welding is one of the most used joining processes, good understanding of the factors that affect the quality of welded joints is critical. Due to the heat generated by the arc between the electrode and the base material, changes occur in the microstructure of the base material that can manifest as modification of grain size, dissolution and/or precipitation of secondary phases, inhomogeneity, occurrence of cracks, and other types of defects, whereby the reliability and load-carrying capacity of the welded component decreases. As the present defects might not be detectable by visual and nondestructive inspection methods, the mechanical properties of weld joints must be verified at least by tensile tests, hardness measurements, but impact toughness tests, fracture toughness test and in the case of dynamic loads, also fatigue tests is required. Improvements in mechanical properties and the study of crack behavior of dynamically loaded materials and weld joints in a variety of steel types has attracted the attention of numerous authors [1, 2, 3, 4].

In weld joint consumable material and a part of a base material are melted and solidified into weld metal during the cooling. The heat input needed for welding increases material temperature in the vicinity of the weld metal. As result of heat input some transformation in microstructure will occur at high heated area of base material which is not melted [1, 2], this region known as heat affected zone (HAZ) of the weld joint. Heat affected zone (HAZ) microstructures is very inhomogeneous and complex, its microstructure usually consist of Coarse Grain HAZ, Fine Grain HAZ, Inter Critical HAZ and Over Tempered HAZ. The part of the HAZ which is heated the most is located near to the fusion zone, therefore crystal grains are coarsening during due to long period time of the thermal cycle. The coarse grain microstructure, called the coarse grain heat affected zone (CG HAZ), the fine grain microstructure (FG HAZ) is the next sub-region of HAZ results from this process; see Figure 1.

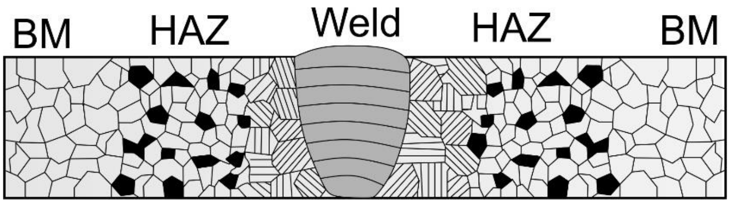

Figure 1. Welded joint; BM (base material), HAZ (heat affected zone), WM (weld material)

Behavior of the material during process of welding in the view of the metallurgical aspect and metastable phase diagram Fe-C is shown in the Figure 2.

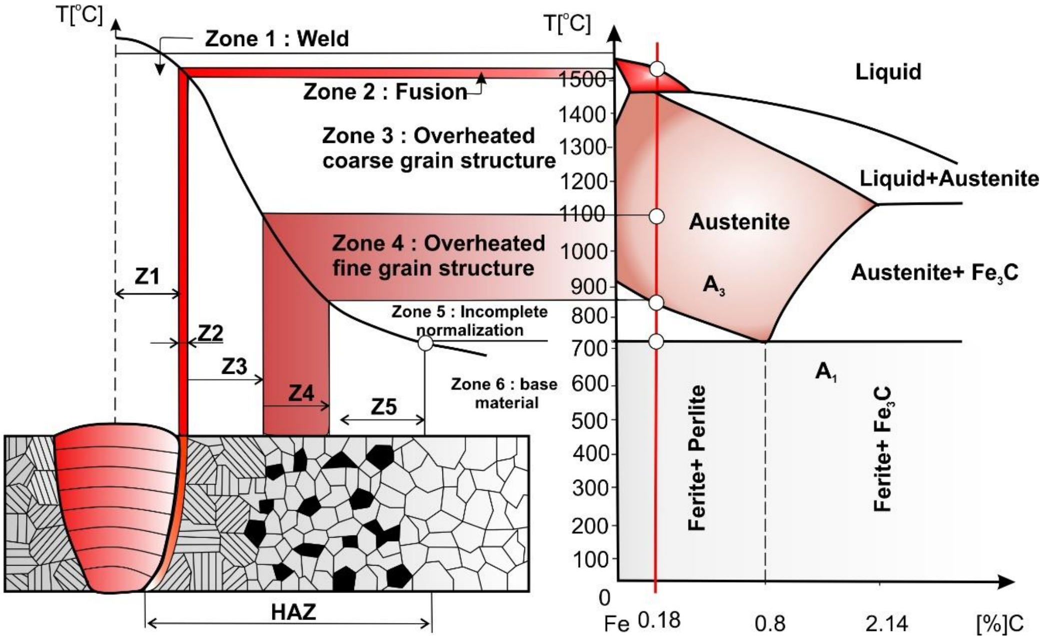

Figure 2. S235JR steel behavior during welding

2 Material and methods

S235JR describes non-alloy structural steels and falls in Part 2 of the EN 10025 specification [5]. The 'S' denotes a 'structural steel' with a yield strength of 235 MPa. The 'JR' designation confirms that the material has undergone a Charpy V-notch impact test at 27 joules at room temperature. Chemical composition and mechanical properties of the steel are shown in Tables 1 and 2.

Table 1 Chemical composition of the steel (weight /%)

C	Mn	Si	S	P	N
0,17-0.2	1.50	0,030	0,045	0,045	0.014

Table 2 *Mechanical properties of the steel*

$Rp_{0.2}$ / MPa	R_m / MPa	A_5 / %
235	510	26

2.1 Experimental methods

Plates with the thickness of 8mm and length of 300mm are welded together using metal inert gas (MIG) welding method. The welding parameters were: Intensity I=98A, tension U=25V, and the welding speed was v=26.32 cm/min. From the welded plate are specimens taken for the investigation of the mechanical properties. The parameters are summarized in Table 3.

Table 3. Welding parameters for real welding.

I/A	98
U/V	25
$v_{welding}$/cm min^{-1}	26.32
Q/kJ cm^{-1}	4.75
Wire/ electrode	ϕ2.5mm
$\Delta t_{8/5}$/s	5

Tensile tests were performed with a universal servo-hydraulic testing machine (INSPECT 100), according to the standard EN ISO 6892-1, 2009 method B [6]. Standardized rectangular specimens were used, with a thickness of ao=8 mm, width bo=14mm and a gauge length of Lo=50 mm.

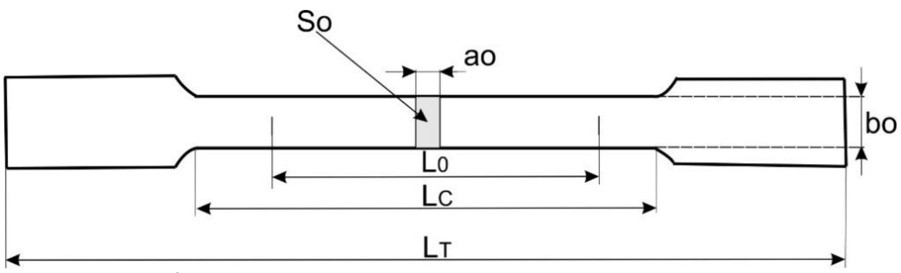

Figure 3. Geometry of standardized rectangular cross section specimens and tensile test machine

Vickers hardness HV, Brinell hardness HB and Rockwell hardness HRB was measured with a Hartip 3000 Portable Hardness Tester in compliance with standard EN ISO 6507-1 [7].

Figure 4. Position of hardness measurements and Hartip 3000 Portable Hardness Tester

2.2 Numerical methods

SOLIDWORKS Simulation is used as a method to analyze our design, evaluate its performance and make decisions to improve product quality but always in comparison with the results taken from experimental work. The software employs a numerical technique called Finite Element Analysis, or FEA. The concepts behind FEA were developed in the early 1940's, but the method became more mainstream in the 1980's and 90's when it was implemented on desktop computers [8]. Today, FEA is a powerful tool that is widely used by designers across many industries. It's used for solving structural, vibrational and thermal problems virtually before they pose a real problem in reality.
For additional analysis capabilities, SOLIDWORKS offers three simulation packages designed to meet the needs of different users:

- Simulation Standard is used for structural, motion and fatigue analysis of parts and assemblies.
- Simulation Professional adds more capabilities including frequency, thermal, buckling, drop test and optimization studies. It also includes a full set of productivity tools that allow you to work faster and achieve greater accuracy in your results.
- Finally, the Simulation Premium package is capable of analyzing plastic and rubber components, metal forming operations, composite materials, and dynamic loads such as oscillating or vibrating structures.

2.3 Conversion procedure of wind speed into the force and its usage for FEA simulation

When moving air - wind - is stopped by a surface - the dynamic energy in the wind is transformed to pressure. The pressure acting the surface transforms to a force [9]:

$$F_W = p_d \cdot A = \frac{1}{2}\rho \cdot v^2 \cdot A$$

where:
F_W = wind force (N)
A = surface area (m^2)
p_d = dynamic pressure (Pa)
ρ = density of air (kg/m^3)
v = wind speed (m/s)

Note – this is an approximation because in practice wind force acting on a object creates more complex forces due to drag and other effects.

According to the data provided by [10] the maximum wind speed in region of Prishtina was 77.8 km/h or 21.61 m/s and based on this the dynamic force per unit area of Street Lighting Construction can be calculated as:

$$F_W = p_d \cdot A = \frac{1}{2}\rho \cdot v^2 \cdot A$$
$$F_W = \frac{1}{2} \cdot 1.2 \cdot \left(21.61\frac{m}{s}\right)^2 \cdot 0.8(m^2)$$
$$F_W = 224.15 \ [N]$$

Regardless of the specific design being tested, the fundamental steps of any FEA study are always the same. We start with a geometric model. This could be a native SOLIDWORKS part, multi-body part, or an assembly. It could also be a file from another CAD system, or even a neutral format such as a STEP, IGES, or a Parasolid. SOLIDWORKS Simulation is capable of analyzing all of these file types [8].
Next, we assign materials (according to material specification) to all the components, define the loads acting on the structure (for our case was force of magnitude of 224.15 N) and apply restraints to describe how it's anchored or held in place.
Lastly, we approximate the geometry by splitting it into smaller and simpler entities known as elements. This process is called "meshing", and it can be automated by the software. For advanced users who would prefer more control over the meshing process, there are built-in tools that allow for additional refinement.
After running the study, we can view the results using a variety of color plots, graphs, animations and reports which are presented under the results and discussion part.

3 Results and discussion

3.1 Tensile test

Force vs elongation results of tensile test are shown in the diagrams below for three tested specimens, and it is clear that no big difference on the value of maximum tensile strength is founded.

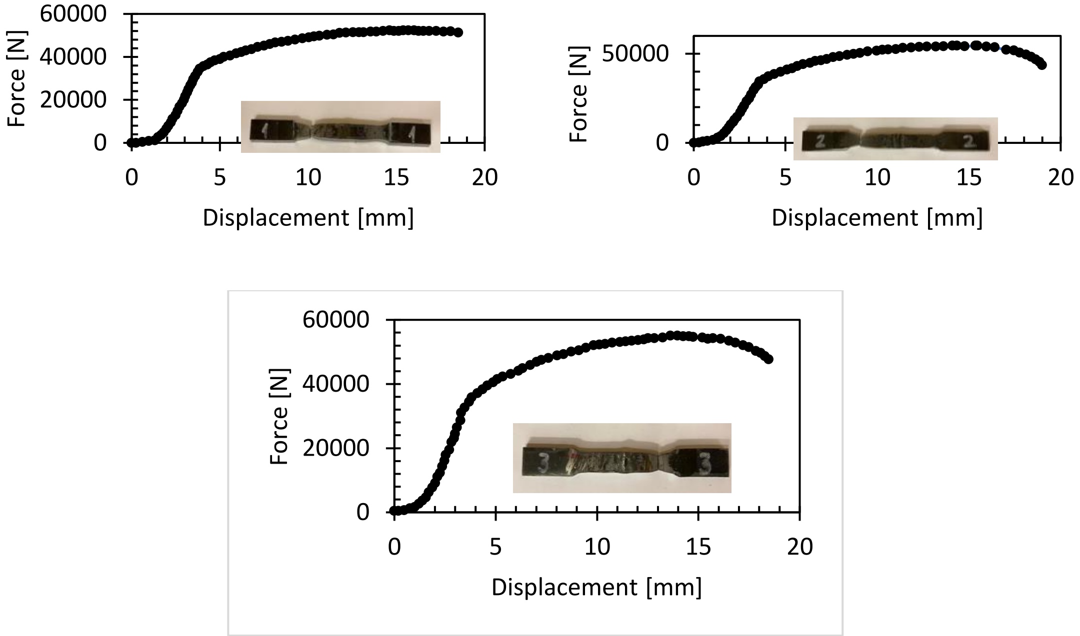

Figure 5. F vs Δl diagrams taken and tested specimen from tensile test machine

All specimens have been fractured outside of the weld bead, which clearly can be distinguished from the diagrams on figure 5. This mean that the welding has been carried out in accordance to the PQR and WPS requirements.

3.2 Hardness measurement

The hardness results are derived after the performing the measurement. At least 15 measurements are performed. The results show that at heat affected zone hardness has tendency to increase due to the change in microstructure.

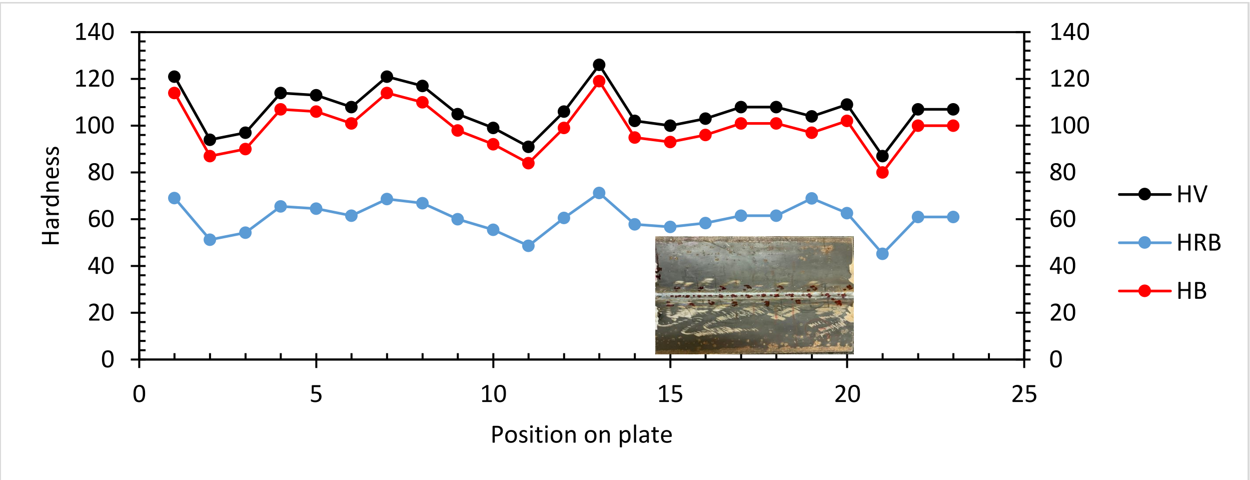

Figure 6. Hardness measurements in longitudinal bead direction

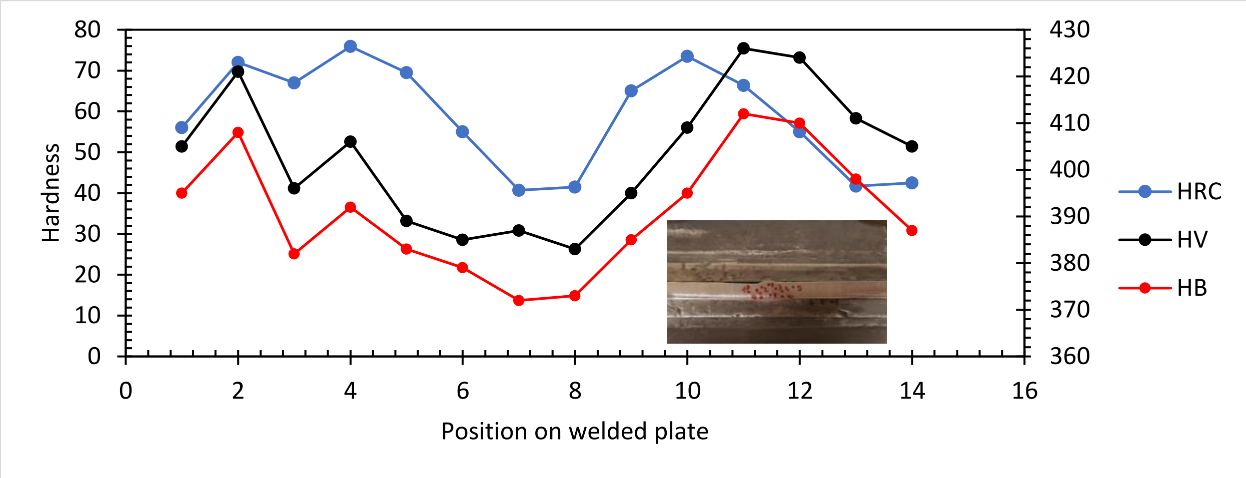

Figure 7. Hardness measurements in frontal bead direction

Measurements presented on figure 7 shows that the hardness number is quite lower in the weld bead (region between 5-9), in the other hand, positions from 5 on left side and up 9 on the right side show tendency to increase the hardness number which practically is the heat affected zone region which is undergone in microstructure transformations and potentially is most risking part to failure of the entire weld joint.

3.3 FEA analysis

After drawing the geometric model of street light on SolidWorks software, the static analysis is performed. First, the material S235JR is assigned to the model, after that the fixture and forces were defined, as well as the mesh grid of the model. Finally, the static analysis has been run and the results are as we can see on the figure 8.

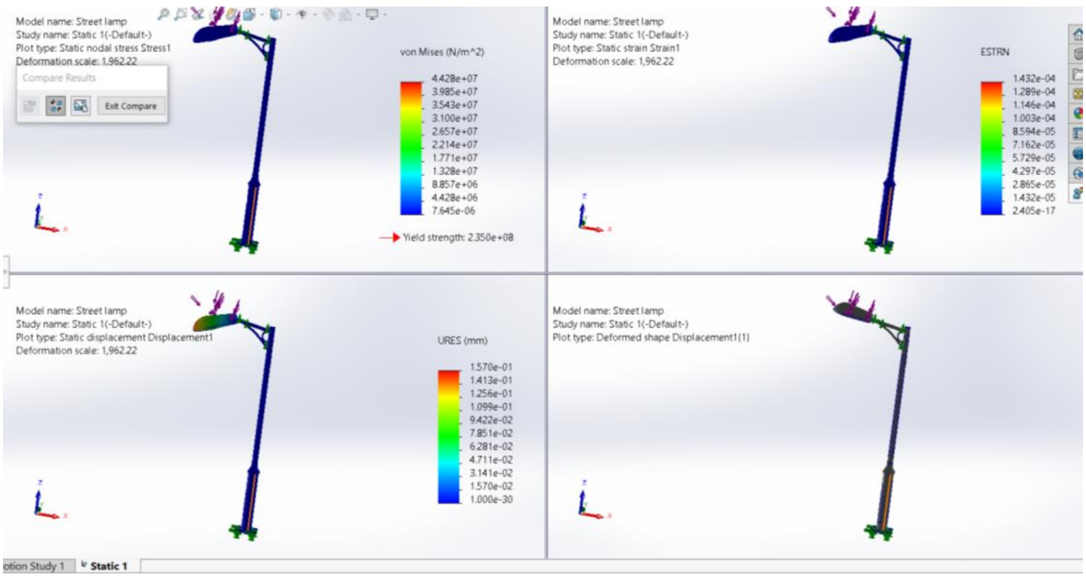

Figure 8. Static analysis performed by SolidWorks

According to the results taken from FEA analysis it is clear that the risk for failure does not exist because the van Misses stress are well below the yield point of the material therefore no concern should be made if the welding is done properly and according to the WPS and PQR specification.

4 Conclusion

The quality of the welded beads is guaranteed and does not present a risk of failure of the welded joint in the bead and in the thermal impact zone.

The strength of the welded beads and the heat affected zone of the welded joint was within the permissible conditions based on the level of the amount of heat input during welding.

During the visual inspection, no visible defects were observed, while after the inspection of the welded beads for the value of the beads and reinforcement, they were in conditions allowed by the ISO 5817:2007 standard.

The static analysis derived from the FEA analysis has confirmed that there is no risk for the welded joint even in cases where we have strong air currents, i.e. in case of strong winds.

5 References

[1] Fidan Smaili, Tomaz Vuherer, Afrim Gjelaj, Besart Berisha, Hajredin Ibishi, "Heat affected zone microstructure of welded joint prepared in artificial manner," in *ICMSER conference, UBT*, Prishtina, 2019.

[2] Shahin Akbarnejad, Investigation on static strength of welded joints, Stockholm, Sweden: Royal Institute of Technology, 2012.

[3] Nadot, Y., " Fatigue from Defect: Influence of Size, Type, Position, Morphology and Loading.," *Int. J. Fatigue ,* Vols. 154, 106531., 2022, .

[4] Mandal, P.; Al Mamun, A.; Da Silva, L.; Lalvani, H.; Perez, M.; Muir, L., " Impact of various heat treatments on the microstructure evolution and mechanical properties of hot forged 18CrNiMo7-6 steel.," in *In Proceedings of the 29th ASM Heat Treating Society* , Columbus, USA, 2017.

[5] BS EN 10025-2:2019, Hot rolled products of structural steels - Part 2: Technical delivery conditions for non-alloy structural steels, Brussel, Belgium: ISO, 2019.

[6] EN ISO 6892-1, 2009 method B. , Metallic materials — Tensile testing — Part 1: Method of test at room temperature, Switzerland : ISO, 2009.

[7] EN ISO 6507-1:2018(en),, Metallic Materials—Vickers Hardness Test—Part 1: Test Method. European Committee for Standardization:, Brussels, Belgium,: ISO, 2018..

[8] Alignex, Inc. , "Introduction to SOLIDWORKS Simulation – Finite Element Analysis," Dassault System, 9 Januar 2020. [Online]. Available: https://blogs.solidworks.com/tech/2020/01/introduction-to-solidworks-simulation-finite-element-analysis.html. [Accessed 15 10 2022].

[9] Engineering ToolBox, "Engineering ToolBox, Wind Load vs. Wind Speed. [online] Available at:," 13 10 2011. [Online]. Available: https://www.engineeringtoolbox.com/wind-load-d_1775.html. [Accessed 13 10 2022].

[10] Metrology Agency of Kosovo, "Metrology Agency of Kosovo," 6 3 2007. [Online]. Available: https://amk.rks-gov.net/page.aspx?id=2,1. [Accessed 14 10 2022].

Off-Line Part Preparation for Laser Powder Bed Fusion Production

Betim Shabani[1], Fisnik Osmani[2*], Vladimir Dukovski[2]

[1] UBT – Higher Education Institution, Lagjja Kalabria, 10000 Pristina, Kosovo

[2*] University of Mitrovica "Isa Boletini", Ukshin Kovaçica, 40000 Mitrovica, Kosovo

[2] University St. Cyril and Methodius in Skopje, Faculty of Mechanical Engineering, 1000 Skopje, North Macedonia

betim.shabani@ubt-uni.net

fisnik.osmani@umib.net

vladimir.dukovski@mf.edu.mk

Abstract. There are constant improvements in recent years in different manufacturing technologies. One of them is additive manufacturing (AM), specifically metal AM category, laser powder bed fusion (L-PBF). Despite the high range of freedom in design and capability for producing complex parts with this technology, there is a need for the comprehensive study of preparing the parts for production, taking into consideration orientation, and support generation. In this research, the selected parts for investigation have different shapes and are tested in different orientation angles. After the orientation optimization based on three factors: build time, supports volume, and distortion tendency, the optimal solutions for support generation for particular parts were selected. The aim of the work has been to optimize the part preparation based on factors that are important for technical and economic aspects. Further work as a more comprehensive study should employ the simulation analysis (macroscale and mesoscale) as the input for the preparation of the part for L-PBF production.

Keywords: Additive Manufacturing, Laser Powder Bed Fusion, Build Time, Supports Volume, Distortion Tendency.

1 Introduction

The need for simulation is almost everywhere, especially in different fields of engineering [1]. For this reason, simulation processes may vary by application, especially when we need to pre prepare digital CAD model for any of manufacturing processes [2]. Related to recent manufacturing developments [3], one of the most promising is laser powder bed fusion (L-PBF) [4], which is category of metal additive manufacturing (AM) [5]. In this research work the workflow of offline part preparation is presented. This step is important to have more clarification as may cause effects in product development in terms of time, cost and quality.

In Section 2, CAD models for investigation are presented. In Section 3 the part orientation options with optimal solutions are calculated, continued in Section 4 with support structure generation based on best solution. Finally, the conclusions will derive the actual situation and further work.

2 CAD Models Selection

As we know AM accepts only models in digital format [6]. We have decided to choose three models with different geometric shapes. These models are designed in CAD software [7] (Autodesk Inventor) and have real dimensions.

The first model (Figure 1a) is a shaft with several passes where the maximum diameter is 40 mm while the total length is 65mm. The second model (Figure 2b) is an amplifier which has dimensions of 15 x 25 x 60 mm. The third model (Figure 1c) is a more complex mechanical part that has channels and holes. The maximum dimensions are 84 x 94 x 150 mm.

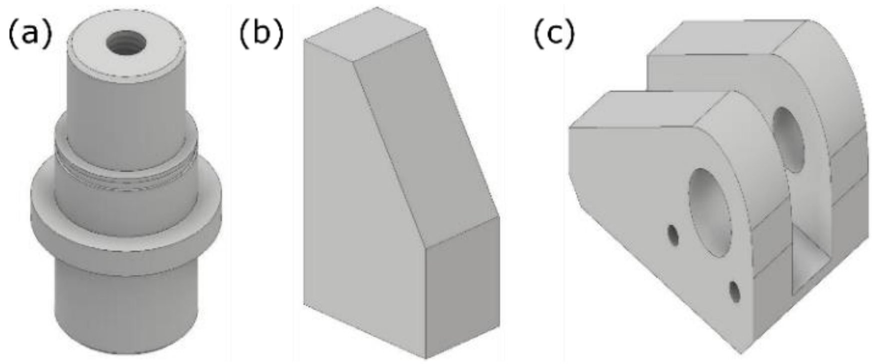

Fig. 1. CAD Models.

3 Part Orientation

Orientation is a very important task in the L-PBF process, especially in the production of metal parts [8]. The relationship with the base plate determines several factors that maximize the efficiency of the entire process, such as: reduction of production time, reduction of material and supports, prevention of detachment from the structure. The selection for the most favorable orientation is done in a qualitative way where each factor is in competition with the other and from this triangle of factors we set the priorities by percentage. After setting the criteria, maps are obtained with the possibilities for orientation. These maps are presented with colors that indicate which of the orientations is better or which should be optimized further. Green color indicates optimal orientation, red indicates not recommended orientation. The combination of these depends on the prioritization for the selected factors presented in percentage. For all three models, the same criteria for prioritization of factors was applied (Figure 2). For all analyses, ANSYS SpaceClaim was employed [10].

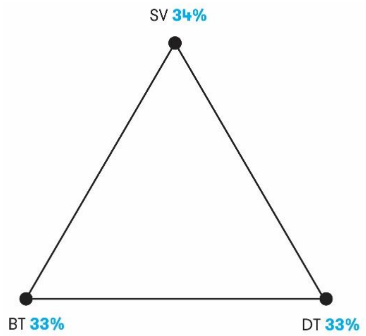

Fig. 2. Triangle of prioritization.

According to Figure 2, build time and distortion tendency are weighted by 33%, while support volume by 34%. Each of these affects the final map where the choice of optimal orientation must be made. Since the division is almost proportional, then for each factor we will have an appearance on the final map. Each model has been tested with three orientations: 0-degree, 45-degree, and 90-degree. The map for model (a) is presented in Figure 3, for model (b) in Figure 4, and for model (c) in Figure 5.

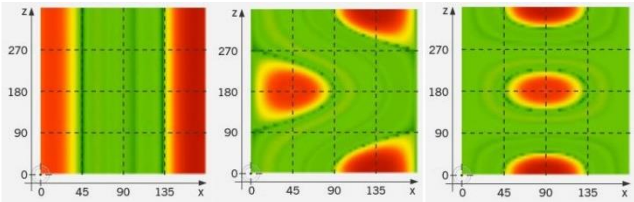

Fig. 3. Optimized area: (left) 0-degree; (middle) 45-degree; (right) 90-degree.

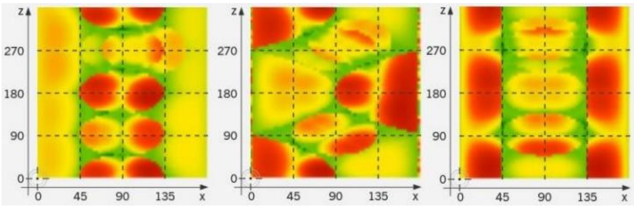

Fig. 4. Optimized area: (left) 0-degree; (middle) 45-degree; (right) 90-degree.

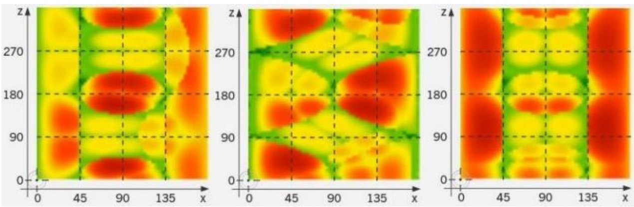

Fig. 5. Optimized area: (left) 0-degree; (middle) 45-degree; (right) 90-degree.

In all cases, the horizontal axis X enables the part to have alternatives from 0 to 180 degrees, while for the vertical axis, which is Z, from 0 to 360 degrees. Through these possibilities, all rotation cases for the respective positions are possible.

4 Support Structures Generation

Since for L-PBF it is required that the part need to be attached to the base plate, the support structures must be specified [9]. First of all, the regions where the supports will be found must be specified. To determine the region, three parameters are considered: overhang angle, region size, and line regions.

Overhang angle: Defines the angle between the part and the baseplate (Figure 6). Any angle defined below the given value will not have support. For our case, 45 degrees was set.

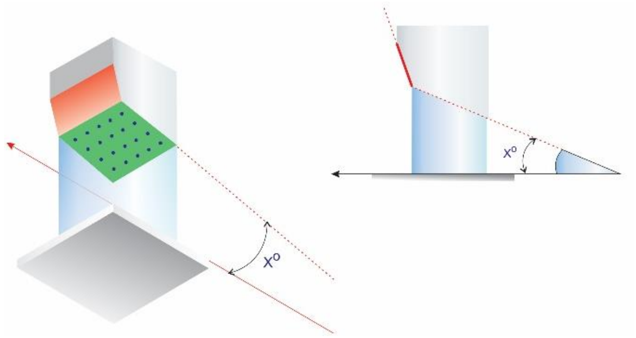

Fig. 6. Overhang angle [11].

Region size: Represents the minimum surface for which supports must be generated (Figure 7). The area smaller than the given value will not be considered for treatment. For our case, 0.1 mm^2 was set.

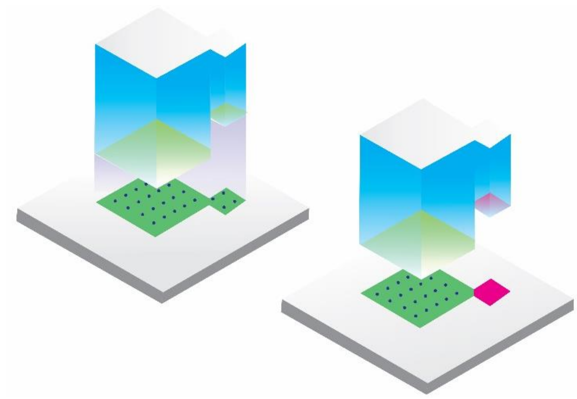

Fig. 7. Region size [11].

Line regions: This enables the generation of supports at the edge of the part and is optional. After defining the parameters mentioned above, the next step is the generation of supports in the regions defined for the respective models. Depending on the model and position, several types of supports can be generated such as: block, heart cell, rod, tree, and contour. Each of these types has its own specifics. In our case, block support and line support were used.

Block support are supports that are recommended to be used in regular geometric shapes and cover the entire space of the selected region. These are used for model (a) for 90-degree orientation and model (c) for 0-degree orientation (Figure 8).

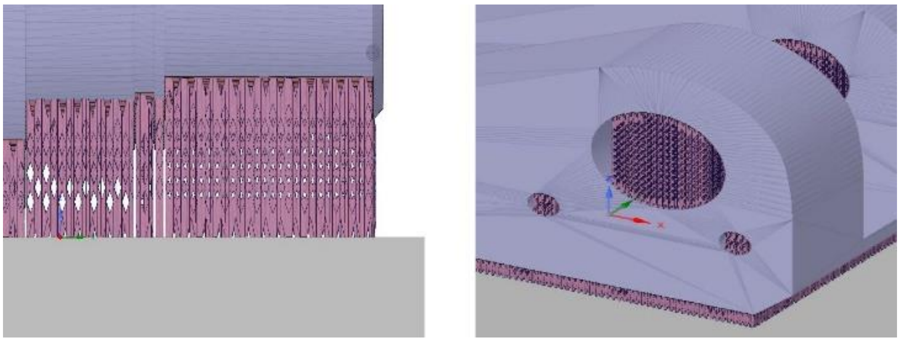

Fig. 8. Block support: (left) Model (a); (right) Model (c).

Line support are used to connect the ends of the part with the baseplate. The lower form which is attached to the baseplate is wider for more stability. Such case is used in model (b) in 45-degree orientation (Figure 9).

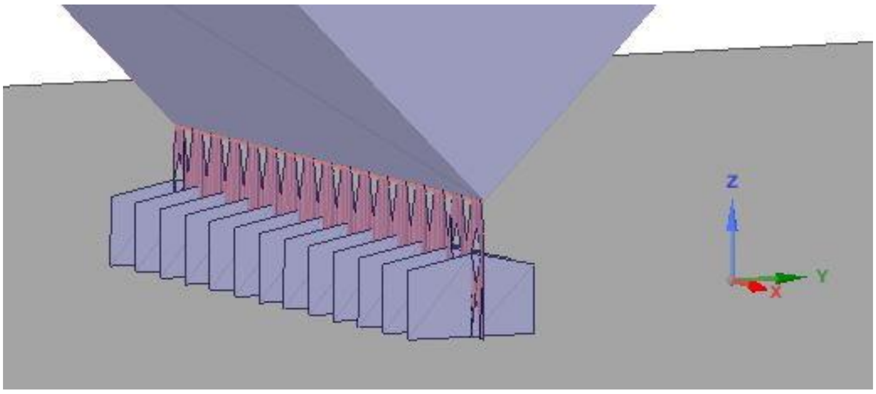

Fig. 9. Line support in Model (b).

In all cases, the distance from the baseplate to the surface that is closest to the part was set at 5 mm, as the possibility of attaching between them.

5 Conclusions

In this paper, we presented some aspects of off-line part preparation for L-PBF. Based on selected models for investigation, optimization for orientation and support structures were analyzed with case study. Related on the research we can conclude:

- The importance of factors: build time, distortion tendency and support volume are critical for achieving the high level of part preparation.
- Based on case studies we can notice that complexity for preparation will increase based on geometry of the part.

Further work can be the multi-level simulation for part preparation including mesoscale and macro scale simulation.

References

1. Madachy, R.J. and D.X. Houston, *What every engineer should know about modeling and simulation*. 2017: CRC Press.
2. Groover, M.P., *Fundamentals of modern manufacturing: materials, processes, and systems*. 2020: John Wiley & Sons.
3. Galantucci, L.M., et al. *Additive manufacturing: new trends in the 4 th industrial revolution*. in *Proceedings of the 4th International Conference on the Industry 4.0 Model for Advanced Manufacturing: AMP 2019 4*. 2019. Springer.
4. Yadroitsev, I., I. Yadroitsava, and A. Du Plessis, *Basics of laser powder bed fusion*, in *Fundamentals of Laser Powder Bed Fusion of Metals*. 2021, Elsevier. p. 15-38.
5. Hansen, H., et al. *Additive manufacturing of metal components–process-material interaction in different process chains*. in *IOP Conference Series: Materials Science and Engineering*. 2019. IOP Publishing.
6. Alfaify, A., et al., *Design for additive manufacturing: A systematic review*. 2020. **12**(19): p. 7936.
7. Tickoo, S., *Autodesk Inventor Professional 2019 for Designers*. 2013: Cadcim Technologies.
8. Leutenecker-Twelsiek, B., C. Klahn, and M.J.P.C. Meboldt, *Considering part orientation in design for additive manufacturing.* 2016. **50**: p. 408-413.
9. Jiang, J., et al., *Support structures for additive manufacturing: a review.* 2018. **2**(4): p. 64.
10. ANSYS SpaceClaim (2020). Retrieved from https://www.ansys.com/it-it/products/3d-design/ansys-spaceclaim
11. ANSYS, Inc., Additive Prep User's Guide (2021). Published in the U.S.A.

Identifying suspicioushuman activity usingartificial intelligence and deep recognition

Vesa Morina1, Shqipe Sejdiu2

1UBT – Higher Education Institution,
Pristina, Kosovo
vesa.morina@ubt-uni.net

2UBT – Higher Education Institution,
Pristina, Kosovo
ss36902@ubt-uni.net

Abstract. Every day we are on the move, we are active during the process of going to work, to studies and for all our daily activities that complete our day. We as human beings always tend to be different from each other, this difference manifests itself with its positive and negative sides. The negative actions of many people have a legal categorization in terms of punishment, but history hastaught us that there are moments and cases when malicious actions are of such alevel that the punishment that can be given to a person for that action is not proportionate with the damage caused. To prevent malicious actions, it has always been invested in technological assets and people who, by monitoring them, could contribute to society to prevent suspicious actions that could bring irreparable consequences and high human losses. Human interest reputation is a critical but difficult topic to study and predict through technological devices. In this paper, we will present the techniques, practices and algorithms used to identify suspicious human activities using artificial intelligence and deep recognition.

Keywords: Activity recognition; Deep learning; Human activities; Artificial intelligence

1 Introduction

Considering the many opportunities offered for solving various problems by integrating artificial intelligence and deep recognition and seeing the unstoppable development of artificial intelligence as an application in various fields, this was also applied to the field of Human Activity Recognition (HAR).
Since Human Activity Recognition (HAR) includes various human activities such as walking, running, sitting, sleeping, standing, showering, cooking, driving, opening the door, abnormal activities, etc., we will try to get the suspicious human activities which are a set of different activities and we will try to identify them, either through the acceptance and analysis of video signals generated by security cameras and also from the data that can be received from different sensors of located in public spaces [1].
The numerous and different incidents everywhere in the world as well as the various cases in the past, such as robberies, starting from local to large banking centers, various problems in the army, government, etc., are factors that push us to come to thesolution of these many problems. In this paper, we will use different Human Activity

Recognition (HAR) methods, including methods that we can use on different sensors, as well as methods applied to video recognition, so that we can train the models with different human activities and come to the desired results [2].

2 Human Activity Recognition - HAR

The field of Human Activity Recognition (HAR) has become one of the most discussed research topics due to the availability of sensors and accelerators, low cost and lower power consumption, direct data transmission, and advances in computer vision. , machine learning, artificial intelligence and IoT. Various human activities that surround us are known through HAR. Data can be collected from sensors located in the environments, accelerometer or through video signals and captured photos.
Through the monitoring of HAR, actions that may lead to crime, the home environment, driving activities as well as military actions can be identified [3].
In human activity recognition systems, various basic level characteristics are introduced to describe the observation of an activity. The SVM (Support Vector Machine) technique is applied to the observation of human movements in a video using the concept of movement classification. SVM is a model for classification and regression problems. The idea of SVM is that the algorithm creates a line or a hyperplane that divides the data into classes [4].
Another proposal is the description of human movement with the help of spatio-temporal bag-of-features (STIP). By using the STIP feature and combining the rich context information that is extracted from the video and using the deep model, this combination is able to capture the extensive information about people's movement and interactions, scale to recognize the activity of each individual in the scene and improve the accuracy of the overall activity recognition task.

3 Human Activity Recognition based on context

Context information is widely used in many video signal analysis applications. In the topic of human activity recognition, many approaches integrate contextual information by proposing new descriptors of features extracted from an individual and the surrounding area. The description of the action context (eng. AC-Action Context) records the activity of the focal point and the behavior of others nearby. The AC descriptor vector with contextual action vectors captures the actions of the surrounding people by comparing it with the surrounding environment. The proposal was a spatio-temporal volume descriptor (STV-Spatio-Temporal Volume), which captures the spatial distribution and movement of individuals in the scene to analyze group activity [5].

4 Deep models for human activity recognition

The deep models that have been used over the years have aimed to identify the actions of individuals separately in a scene or environment where there are more people. As a source of information to start the processing and then extract the identification results, the image generated from the video of six people is represented in the figure below. Unlike other used methods, the deep method aims to identify individuals in the environment where they are surrounded. Similarly, this method uses a deep form version that studies the use of contextual data extracted from human actions in a video scene.
As can be seen in the following picture, the deep model process is represented by several stages starting from receiving the signal to the result of possible human activity [6].

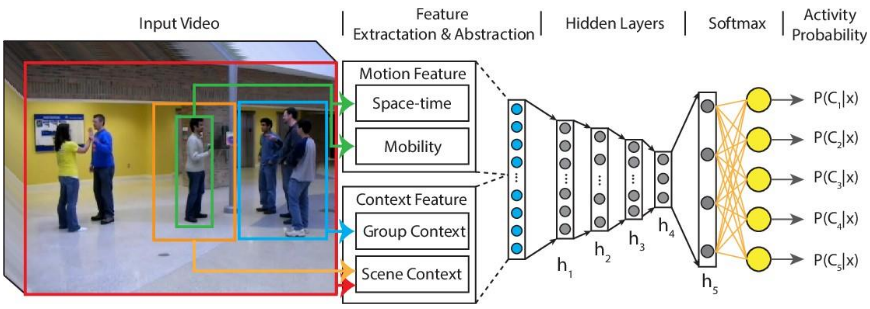

Fig. 1. Deep model process

5 Results

As a process during the automation of monitoring, first the background model or the surrounding environment is taken to create the known model or pattern where then human activity is easily identifiable due to the change in appearance. According to the figure below, the graph and the steps that are taken until a decision is made are presented.

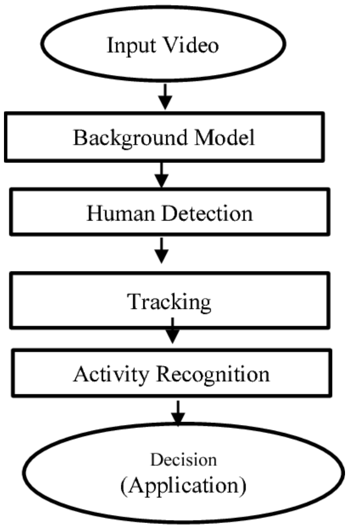

Fig. 2. Steps of human activity recognition

In the following, we have shown the human activities in the two versions obtained from the Collective Activity data.
The first version presents the confusion matrix with 5 activities, such as: pass, wait, queue, walk and talk. The numerical values within the matrix numerically represent the identification of the activity. The higher the value, the more likely it is that the system has correctly detected that human activity, and conversely, if the value is small, then the chances are that that activity is not happening.

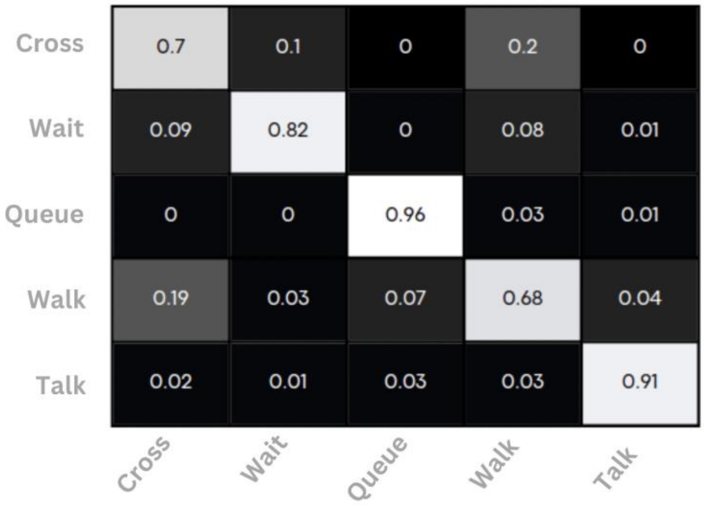

Fig. 3. The first version of Collective Activity

While the second version, which is presented in figure 4, presents 6 activities such as: pass, wait, turn, speak, jump and run. Even in this version, the numerical values represent the same function as figure 3.

Fig. 4. The second version of Collective Activity

Training data is done between the HOG method for human detection. Then the filtering is done which is used to extract the 3D trajectories. To minimize overfitting in the training phrase, the folded data were randomly divided into the validation dataset (30%) and the test dataset (70%). At each parameter update interaction, the accuracy of the validation data set is calculated. When the accuracy on the training data set increases, but the accuracy on the validation data set remains the same or decreases, the neural network is overloaded and will stop training. This model, which was used in both versions of the Collective Activity dataset, integrated motion features as well as multiple sources of context information.

The low value of off-diagonal elements implies that our model is highly discriminative with low decision ambiguity between activities.

In figure 3 and 4, the values obtained by the model with the given dataset are presented in a confusion matrix which visualizes and summarizes the performance of this model.

In Figure 3, the confusion matrix between "Walk" and "Pass" is quite low, and why both activities are part of the "Walk" activity. From the created model, it can be seen in the figures that the walking activity is recognized well enough.
Through the demonstration, the effectiveness of the HAR model is shown, which integrates the motion features (ang. Motion features) and also the variety of information sources (ang. Multiple sources of context information). Also by comparing the accuracy of the SVM classifier and the deep neural network which is trained with the same features we have evaluated the discrimination power of the proposed deep model.
Using the two versions of Collective Activity, the comparison of different models for human cognition and activity has been made. And as a result it is obtained that the deep neural network (DNN) model outperforms the support vector machine (SVM) model with an accuracy of 81.4% in the first version (5 activities) and 91.3% in the second version (6 activities).
And the combined model using deep models, STIP features and context information has obtained quite good results in the two versions of Collective Activity, where we have presented below the accuracy in the 5 activities of the first version as well as in the 6 activities of the second version.

Table 1. Font sizes of headings. Table captions should always be positioned *above* the tables.

The accuracy	Walk	Cross	Queue	Wait	Talk	Jog	Dance	**Average**
Version 1 5 activities	67.6%	70.2%	96.2%	81.6%	91.5%	-	-	**81.4%**
Version 2 6 activities	-	85.4%	97.9%	72.6%	99.6%	96.4%	91.3%	**91.3%**

6 Conclusion and discussion

In conclusion, the aforementioned methods that have been used for the recognition of suspicious human activity using artificial intelligence and deep recognition have been analyzed and we have come to the conclusion that both options, that of recognition based on context and recognition based on in depth models present the current solution to realize the HAR with the current computing equipment and capacities. Also as further work that can be carried out in this area through research could be: What would be the benefits and methods to realize a structure which would be usable and shared by states and organizations security in order to prevent or detect suspicious human activities.

References

1. C. Jobanputra, J. Bavishi, and N. Doshi, “Human Activity Recognition: A Survey”, Procedia Computer Science, 2019
2. C. A. Ronao and S.-B. Cho, "Human activity recognition with smartphone sensors using deep learning neural networks”, Expert Systems with Applications, 2016
3. Wei, Li, and Shishir K. Shah., "Human Activity Recognition using Deep Neural Network with Contextual Information", VISIGRAPP, 2017
4. A. Kushwaha, A. Khare, and P. Srivastava, “On integration of multiple features for human activity recognition in video sequences”, Multimedia Tools and Applications, 2021
5. S. Mekruksavanich and A. Jitpattanakul, “Biometric User Identification Based on Human Activity Recognition Using wearable Sensors: An Experiment Using Deep Learning Models”, Electronics, 2021
6. S. Habib et al., “Abnormal Activity Recognition from Surveillance Videos Using Convolutional Neural Network”, 2021
7. Babiker, Mohanad & Khalifa, Othman & Htike, Kyaë & Hashim, Aisha & Zaharadeen, Muhamed, “Automated daily human activity recognition for video surveillance usingneural

network", IEEE 4th International Conference on Smart Instrumentation,Measurement and Application, 2017

8. I. U. Khan, S. Afzal, and J. w. Lee, "Human Activity Recognition via Hybrid Deep Learning Based Model", 2022

Cataloging in Publication – (CIP)

National Library of Kosovo "Pjeter Bogdani"

621(496.51) (062)

Proceedings International Conference: proceedings of the 11th UBT Annual International Conference: international Conference on Mechatronics, System Engineering and Robotics / edited by Edmond Hajrizi. - Pristina: UBT, 2023. - 32 f.: ilustr.; 30 cm.

1**.** Hajrizi, Edmond

ISBN 978-9951-550-87-1

INTERNATIONAL CONFERENCE ON BUSINESS,TECHNOLOGY AND INNOVATION

CHAPTERS:

- Computer Science and Communication Engineering
- Management, Business and Economics
- Mechatronics, System Engineering and Robotics
- Energy Efficiency Engineering
- Information Systems and Security
- Architecture – Spatial Planning
- Civil Engineering, Infrastructure and Environment
- Law
- Political Science
- Journalism, Media and Communication
- Food Science and Technology
- Pharmaceutical and Natural Sciences
- Design
- Psychology
- Education and Development
- Fashion
- Music
- Art and Digital Media
- Dentistry
- Medicine & Nursing

Lagjja Kalabria p.n KS - 10000, Prishtinë
+383 38 541 400
+383 38 542 138

www.ubt-uni.net
conferences@ubt-uni.net

ISBN 978-9951-550-87-1